CORE
Metadata, citation and similar papers at core.ac.uk
Provided by RERO DOC Digital Library

WOX5–IAA17 Feedback Circuit-Mediated Cellular Auxin Response Is Crucial for the Patterning of Root Stem Cell Niches in *Arabidopsis*

Huiyu Tian[a,2], Krzysztof Wabnik[b,2], Tiantian Niu[a], Hanbing Li[c], Qianqian Yu[a], Stephan Pollmann[d,e], Steffen Vanneste[b], Willy Govaerts[f], Jakub Rolčík[g], Markus Geisler[h], Jiří Friml[b,i], and Zhaojun Ding[a,b,1]

a The Key Laboratory of Plant Cell Engineering and Germplasm Innovation, Ministry of Education, School of Life Sciences, Shandong University, Shanda Nanlu 27, Jinan 250100, China
b Department of Plant Systems Biology, VIB and Department of Plant Biotechnology and Bio-informatics, Ghent University, B-9052 Gent, Belgium
c Department of Biochemistry, University of Missouri, Columbia, MO, USA
d Ruhr-Universität Bochum, Lehrstuhl für Pflanzenphysiologie, 44801 Bochum, Germany
e Present address: Centro de Biotecnología y Genómica de Plantas (UPM–INIA), Campus de Montegancedo, 28223 Pozuelo de Alarcón, Madrid, Spain
f Department of Applied Mathematics and Computer Science, Ghent University, 9000 Gent, Belgium
g Laboratory of Growth Regulators, Centre of the Region Haná for Biotechnological and Agricultural Research and Faculty of Science, Palacký University, 78371 Olomouc, Czech Republic
h Department of Biology, Plant Biology, University of Fribourg, 1700 Fribourg, Switzerland
i Institute of Science and Technology Austria (IST Austria), 3400 Klosterneuburg, Austria

http://doc.rero.ch

ABSTRACT In plants, the patterning of stem cell-enriched meristems requires a graded auxin response maximum that emerges from the concerted action of polar auxin transport, auxin biosynthesis, auxin metabolism, and cellular auxin response machinery. However, mechanisms underlying this auxin response maximum-mediated root stem cell maintenance are not fully understood. Here, we present unexpected evidence that WUSCHEL-RELATED HOMEOBOX 5 (WOX5) transcription factor modulates expression of auxin biosynthetic genes in the quiescent center (QC) of the root and thus provides a robust mechanism for the maintenance of auxin response maximum in the root tip. This WOX5 action is balanced through the activity of indole-3-acetic acid 17 (IAA17) auxin response repressor. Our combined genetic, cell biology, and computational modeling studies revealed a previously uncharacterized feedback loop linking WOX5-mediated auxin production to IAA17-dependent repression of auxin responses. This WOX5–IAA17 feedback circuit further assures the maintenance of auxin response maximum in the root tip and thereby contributes to the maintenance of distal stem cell (DSC) populations. Our experimental studies and *in silico* computer simulations both demonstrate that the WOX5–IAA17 feedback circuit is essential for the maintenance of auxin gradient in the root tip and the auxin-mediated root DSC differentiation.

Key words: *WOX5*; auxin maximum; *IAA17/AXR3*; root patterning; computer simulation.

INTRODUCTION

Dose-dependent cellular auxin responses are central to cell growth and cell fate specification during embryonic and post-embryonic plant development (Kepinski and Leyser, 2005). The primary root development requires both the establishment and maintenance of auxin response maximum in the distal root tip (Vanneste and Friml, 2009). This auxin response maximum is determined by the concerted action of polar auxin transport, auxin production, auxin metabolism (Ljung et al., 2005; Woodward and Bartel, 2005; Stepanova et al., 2008; Tao et al., 2008; Petersson et al., 2009; Grunewald and Friml, 2010) and auxin response machinery (Vernoux et al., 2011). It is essential to control cell division, cell expansion, and stem cell differentiation (Benjamins and Scheres, 2008; Cruz-Ramirez et al., 2012).

Recent theoretical studies suggest the prominent 'reflux loop' hypothesis (Grieneisen et al., 2007; Cruz-Ramirez et al., 2012) that envisions polar auxin transport as a sufficient

[1] To whom correspondence should be addressed. E-mail dingzhaojun@sdu.edu.cn, tel. +8653188362351.

[2] These authors contributed equally to this work.

organizer of auxin response maximum in the QC cells of the root. In contrast, the eminent role of local auxin production in both the establishment and maintenance of the root-associated auxin maximum has been recently postulated (Stepanova et al., 2008; Tao et al., 2008; Ikeda et al., 2009), highlighting the importance of this process for the auxin-maximum guided root patterning. However, developmental cues underlying the regulation of local auxin production in plants remain scarce.

The WOX5 transcription factor is an important member of the WUSCHEL family of plant stem cell regulators that is specifically expressed in the root QC cells to regulate the activity of distal stem cell (DSC) niches (Sarkar et al., 2007). Moreover, the specific WOX5 expression in QC largely relies on IAA17-dependent repression of auxin response machinery since the WOX5 expression was expanded to the endodermis/cortex initials in *axr3-1* (Ding and Friml, 2010). Here, we demonstrate that WOX5 modulates the expression of key auxin biosynthetic genes in the QC cells and thus feeds back on the establishment and maintenance of auxin response maximum in these cells through IAA17-dependent repression of cellular auxin responses. The IAA17-dependent auxin signaling response was also found to be involved in the free IAA production via the regulation of the expression of key auxin biosynthetic gene TAA1 (Stepanova et al., 2008), and thus contributes to the establishment and maintenance of auxin response maximum in QC. Using combined *in vivo* and *in silico* studies, we demonstrate that this previously uncharacterized feedback mechanism links the maintenance of auxin response gradient in the root tip with the graded patterning of the DSC niches.

RESULTS

Polar Auxin Transport Might Not Be Sufficient to Explain Auxin Accumulation in QC Cells

Computer modeling is a commonly used tool to understand the dynamics of auxin distribution in the root development (Swarup et al., 2005; Laskowski et al., 2008; Cruz-Ramirez et al., 2012). The role of polar auxin transport in coordinating the position of auxin response maximum in the root is well established (Blilou et al., 2005; Grieneisen et al., 2007; Vanneste and Friml, 2009). Notably, a localized auxin production largely contributes to this process (Stepanova et al., 2008; Ikeda et al., 2009).

To test the minimal mechanistic requirements for the establishment and maintenance of auxin response maximum in the root tip, we initially used computer simulation approaches based on a simplified version of the 'reflux loop'-root model (Grieneisen et al., 2007). Our model neglects auxin gradients within the cell and in the extracellular space yet captures essential features of a proposed 'reflux loop' transport mechanism (Figure 1A) (Grieneisen et al., 2007). Similarly to the model proposed by Grieneisen et al., we modeled the auxin influx as one effective permeability parameter to capture both free auxin diffusion and AUX/LAX-mediated auxin influx to the cell (Bennett et al., 1996). Given an eminent role of auxin efflux carriers in the polar distribution of auxin, we additionally assumed non-polar localizations of AUX/LAX influx carriers (Swarup et al., 2005). However, a possibility for polarized auxin influx would be an interesting subject for future studies.

The crucial assumption of the 'reflux loop' model is the fixed inward orientation of PIN-FORMED (PIN) auxin efflux transporters in the epidermis and cortex cells (Figure 1A) (Grieneisen et al., 2007). This elegant model predicts an efficient transport of auxin from outer to inner root tissues and the subsequent accumulation of auxin in the QC cells (Figure 1C) (Grieneisen et al., 2007). However, these inward-oriented PIN localizations in the epidermis and cortex tissues assumed in the 'reflux loop' model are not observed experimentally (Kleine-Vehn and Friml, 2008). Instead, PIN proteins largely localize to the apical side of epidermis cells and to the basal-outer lateral side of cortex cells (Figure 1B and 1G) (Kleine-Vehn and Friml, 2008; Wabnik et al., 2011), indicating the clear separation of shootward and rootward auxin fluxes ('flux separation' model) (Figure 1B).

We tested whether the correction of PIN protein localization in the 'reflux loop model' based on these experimental observations (Kleine-Vehn and Friml, 2008) would eventually affect model predictions. Notably, we found that our 'flux separation' model could not reproduce an auxin accumulation in the QC cells that is observed experimentally (Figure 1D) (Blilou et al., 2005), regardless of auxin transport rates (Supplemental Figure 1A–1C). Additionally, the predicted profile of auxin distribution was eventually flat and the predicted auxin maximum has shifted to collumella cells behind the QC center (Figure 1E) that has not been observed experimentally (Blilou et al., 2005).

Taken together, these model predictions might indicate the possibility for additional cues acting together with polar auxin transport to establish and maintain an auxin response maximum in the QC cells.

QC-Localized Auxin Signaling Maximum Requires the Activity of IAA17 Auxin Response Repressor

Predictions from the computer model suggest that mechanisms of auxin accumulation and subsequent auxin signaling in the QC cells may involve additional cues, at least partially independently of polar auxin transport. Good candidates for such developmental signals are QC-localized auxin production (Stepanova et al., 2008; Ikeda et al., 2009) and the local activity of auxin response machinery (Vernoux et al., 2011).

To test these two possibilities, we first addressed the involvement of canonical AUX/IAA auxin response repressors (Chapman and Estelle, 2009) in the regulation of auxin responsiveness in the QC cells. Amongst these AUX/IAA repressors, the IAA17 has a partial expression domain

http://doc.rero.ch

http://doc.rero.ch

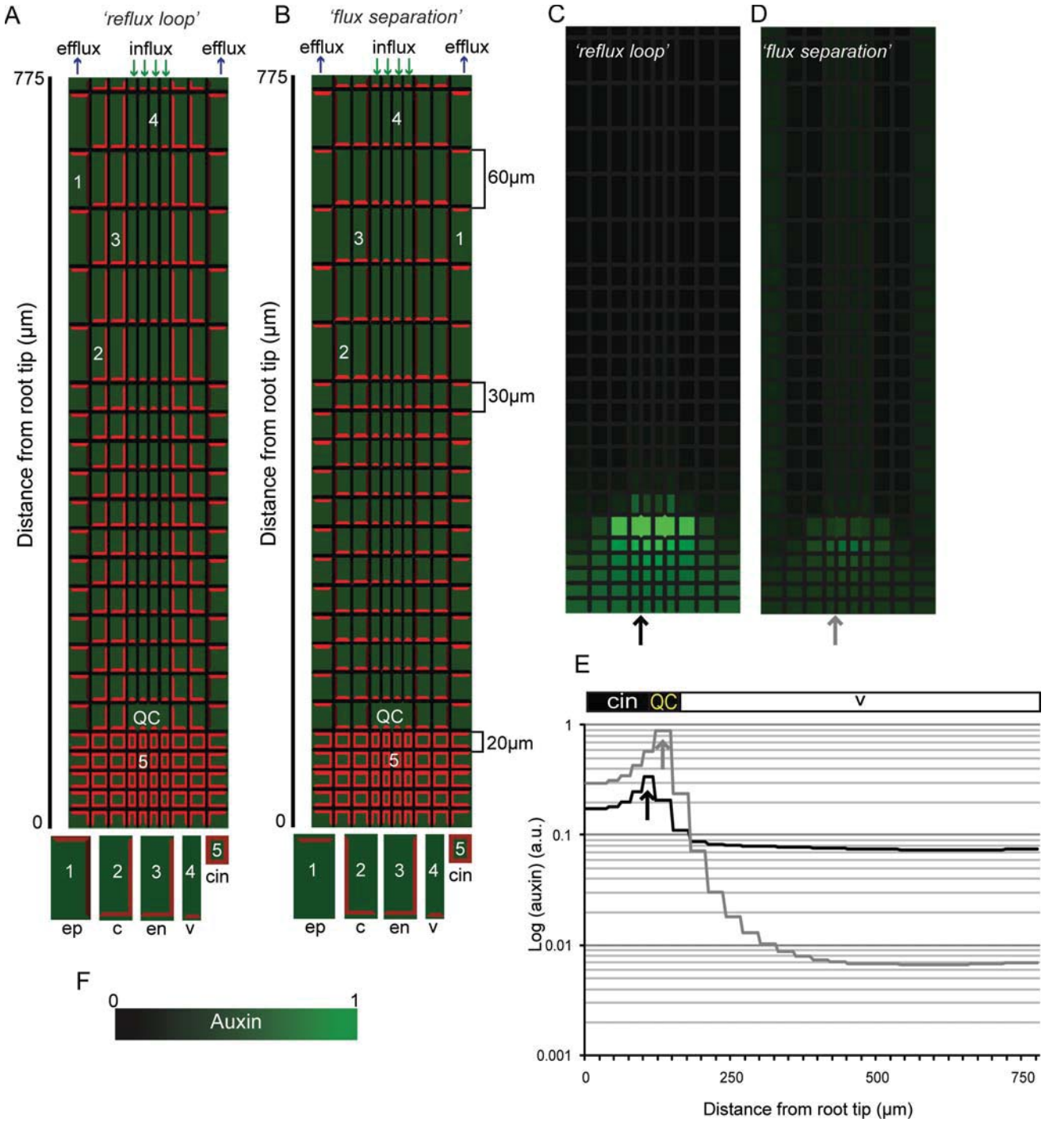

Figure 1. Comparison of 'Reflux Loop' and 'Flux Separation' Models.

(A) The schematic implementation of 'reflux loop' model proposed by Grieneisen et al. (2007). Five distinct regions of the root meristem were incorporated into the model: one layer of root epidermis (1, ep), one layer for both root cortex and endodermis (2,c and 3, en), four central layers of vascular cells (4, v), and columella initials (5, cin). Two QC cells correspond to the most distal vascular cells (4, v).

(B) The schematic implementation of the same root model as in (A) but with experimentally derived PIN2 polarities. Note the substantial differences in PIN2 localization assumptions between 'reflux loop' (Grieneisen et al., 2007) (A) and the 'flux separation' (B) models. In our simulations, only the distal part of the root elongation zone is considered in which PIN2 localizations in cortex cells do not undergo switch to the apical side of the cell.

(C, D) Simulations of 'reflux loop' model demonstrate the efficient auxin reflux through cortex and endodermis tissues that leads to preferential auxin accumulation in the QC cells of the root. In contrast, the simulations of the 'flux separation' model did not predict the auxin maximum in the QC cells.

overlapping with the QC cells (Supplemental Figure 2A–2F). We next used *DR5rev::GFP* synthetic auxin response reporter (Friml et al., 2003) to analyze mutants impaired in IAA17 function (Figure 2). The IAA17 gain-of-function (*axr3*) mutant displayed a highly reduced *DR5rev::GFP* signal in the root tips, with an exception of the QC cells, where the *DR5rev::GFP* signal was more pronounced than that of control plants (Figure 2B). In contrast, the activated version of IAA17 (*35S::VP16-IAA17mImII* mutant) (Li et al., 2009) showed a significant increase of *DR5rev::GFP* signal (Figure 2C) in root tips compared to that of controls (Figure 2A). Moreover, the auxin response maximum was eventually shifted from the QC cells towards columella cells (Figure 2C and 2D) similarly to that predicted by our model (Figure 1D), indicating that proper IAA17 function is required for the maintenance of auxin response maximum in QC.

To substantiate on these findings, we engineered the HA-IAA17mImII (inactivated version of IAA17, mimics gain-of-function mutant *axr3-1*) plants that showed reduced auxin responses (Li et al., 2009) specifically in QC under the

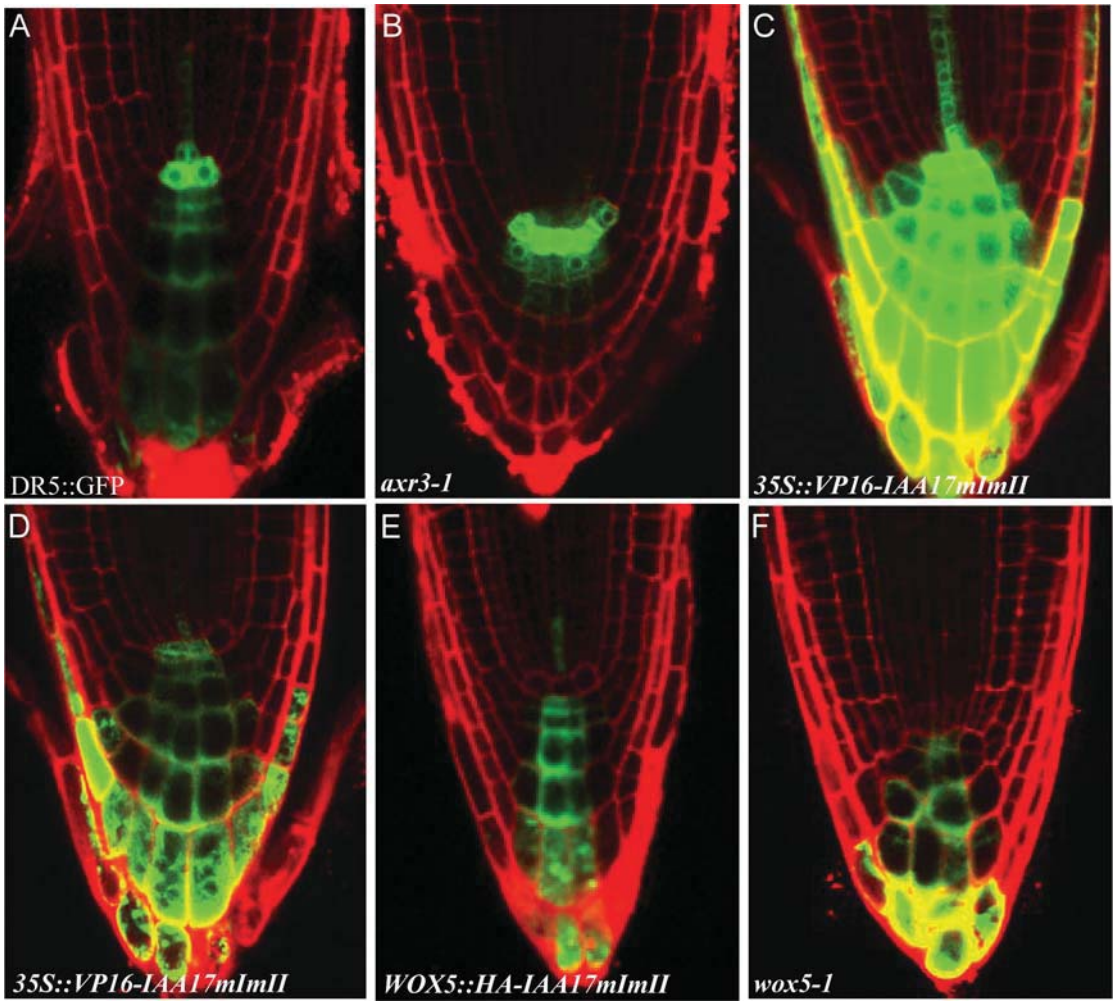

Figure 2. IAA17-Dependent Cellular Auxin Response in the QC.

(A) Localization of the auxin response maximum in the QC cells shown with *DR5rev::GFP*.
(B) The strong auxin response in the QC cells and highly inhibited auxin response of *axr3-1*, shown by *DR5rev::GFP*.
(C) The enhanced *DR5rev::GFP* signals in the whole root tips of the gain-of-function IAA17 mutant (*35S:VP16-IAA17mImII*); the absence of auxin response maximum in QC cells was observed which was shown with the same image captured with reduced laser power **(D)**.
(E) The highly inhibited auxin response in QC cells of the gain-of-function IAA17 mutant (*WOX5::HA-IAA17mImII*), shown by *DR5rev::GFP*.
(F) *DR5rev::GFP* signal in the *wox5* mutant shows similar characteristics to *35S:VP16-IAA17mImII* in the case of the auxin gradient.

(E) Steady-state auxin concentration profiles along longitudinal sections through the vascular and columella tissues (distance from root tip in μm). Steep exponential auxin gradients were observed between QC cells and columella initials (cin) in 'reflux loop' model (black) but not in the model that integrates experimental PIN2 localizations (gray).
(F) Green color coding for relative auxin concentrations. Colors of arrows in (C) and (D) correspond to the colors of auxin gradient profiles in (E).

http://doc.rero.ch

QC-specific *WOX5* promoter (*WOX5::HA-IAA17mImII*). We found that *WOX5::HA-IAA17mImII* plants showed substantial reduced of *DR5rev::GFP* signals in the QC cells (Figure 2E), indicating that QC-localized IAA17 activity is likely to participate in the maintenance of high auxin responses in the QC cells.

Optimal, IAA17-Dependent Auxin Signaling in QC Is Required for Root Distal Stem Cell Maintenance

Our studies suggest a prominent role of IAA17-dependent repression of auxin responses in the maintenance of auxin response maximum in QC (Figure 2). To further figure out the role of IAA17-dependent auxin response maximum in maintaining root DSC identities, we examined *WOX5::HA-IAA17mImII* lines which showed highly enhanced auxin signaling responses specifically in QC. We found that, similarly to the *35S::VP16-IAA17mImII* line, *WOX5::HA-IAA17mImII* also displayed highly promoted root DSC differentiation when compared to wild-type plants (Figure 3A–3C). However, the *axr3-1* mutant, which also showed a sharper QC-localized auxin signaling maximum in QC, displayed highly inhibited DSC differentiation which was shown by multiple layers of DSCs (Ding and Friml, 2010) (Figures 2B and 3E). Our studies indicated that either increased or decreased auxin signaling via manipulating the function of IAA17 protein impaired the maintenance of root DSC identity. Therefore, the patterning of root DSC might rely on the position of auxin response gradient within the root tip which is balanced by IAA17-dependent repression of auxin responses.

WOX5 Modulates Free Auxin Production and Restricts Its Own Expression via IAA17-Dependent Feedback Regulation

Our experimental data indicate that IAA17-dependent auxin signaling responses contribute to the maintenance of auxin

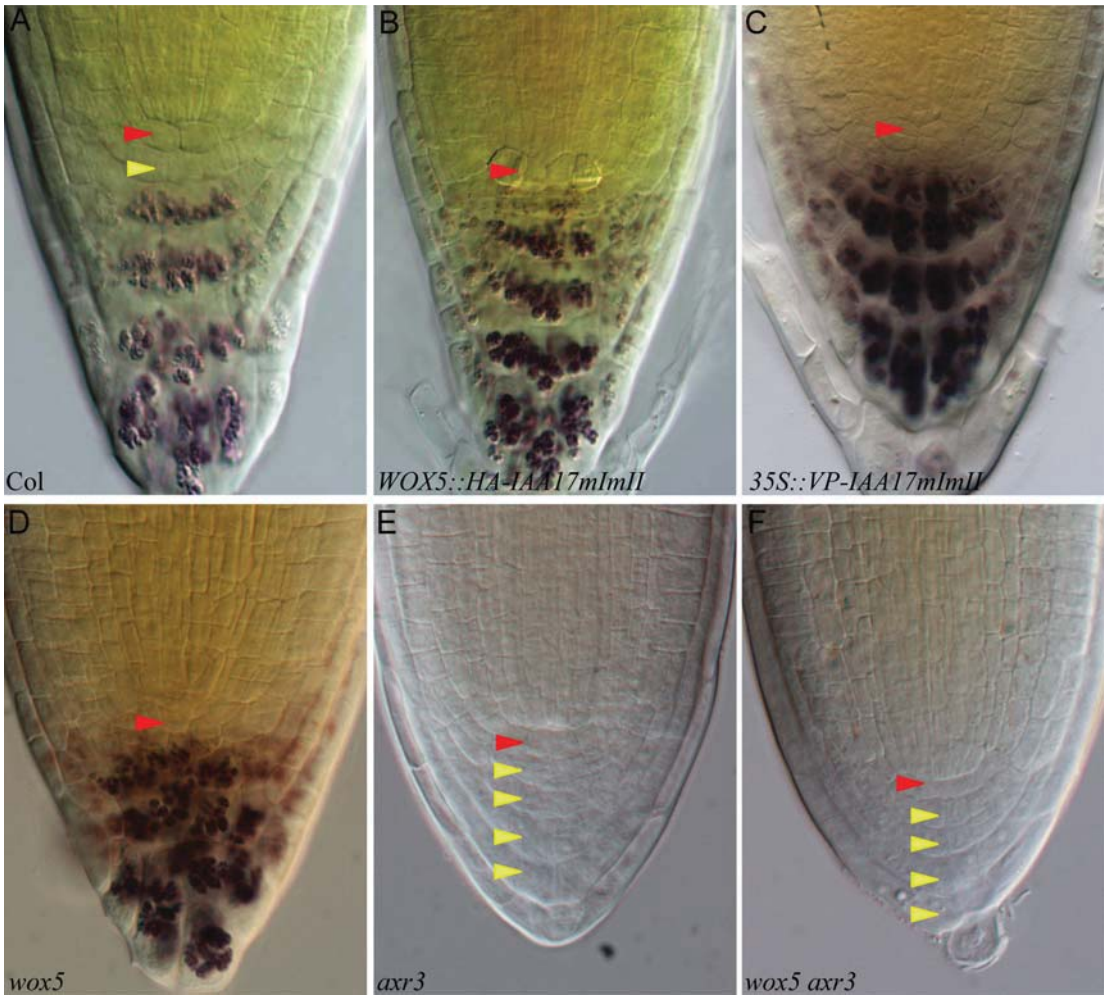

Figure 3. Manipulating IAA17-Dependent Auxin Signaling Influences Root DSC Differentiation.

(A–F) Differentiation status of root DSCs (yellow arrowhead) below the QC (red arrowhead) in 4-day-old seedlings as inferred from the Lugol staining. Wild-type roots show typically one tier of root DS cells (A), *WOX5::HA-IAA17mImII* (B), *35S:VP16-IAA17mImII* (C), and *wox5* (D) all yielded complete root DSC differentiation. Both *axr3-1* (E) and *wox5 axr3* (F) mutants showed similar defects in root DSC differentiation as revealed by multiple tiers of DS cells (F).

http://doc.rero.ch

maximum in the QC cells and thereby the patterning of root DSC niches. Interestingly, the IAA17-dependent repression of auxin responses in the QC cells is required to promote the activity of WOX5 transcription factor (Ding and Friml, 2010). Notably, *WOX5* and *IAA17* expression patterns seem to largely overlap with respect to the QC cells (Supplemental Figure 2A–2F) (Ding and Friml, 2010).

To test the possibility of a feedback loop between IAA17 and WOX5 in the regulation of auxin responses in the QC cells, we analyzed the expression of *DR5rev::GFP* reporter in the *wox5* loss-of-function mutant. We found that the maximum of *DR5rev::GFP* signal was impaired in this mutant (Figure 2F), similarly to that of *35S::VP16-IAA17mImII* line (Figure 2C and 2D), hinting at a possible role of WOX5 in the maintenance of the auxin maximum in the QC. Moreover, *wox5* mutant plants resembled the promoted root DSC differentiation phenotype of *35S::VP16-IAA17mImII* plants (Figure 3C and 3D) that could be rescued by introducing *axr3-1* into *wox5* (Figure 3D–3F). These findings hint on the possible link between WOX5 activity and the IAA17-dependent repression of auxin responses in the QC cells.

To further complement our observations, we studied *WOX5* expression in *35S::VP16-IAA17mImII* and *axr3-1* plants using *WOX5::ERGFP* reporter (Figure 4A–4C). Notably, *WOX5* expression was significantly down-regulated in *35S::VP16-IAA17mImII* (Figure 4B) but not in the *axr3-1* mutant that displayed broader *WOX5::ERGFP* expression domain (Figure 4C) than that of the control (Figure 4A). Notably, this expanded expression of WOX5 in *axr3-1* correlated with reminiscent, ectopic up-regulation of *DR5rev::GFP* signals in endodermis/cortex initials (Figure 2F). Our genetic analysis demonstrates that *WOX*5 and *IAA17* act in the same regulatory pathway (Figure 3D–3F), highlighting the possibility for the feedback regulation between these genes.

To investigate potential mechanisms by which WOX5 contributes to the regulation of auxin response maximum in the QC cells, we tested whether WOX5 could modulate either auxin transport or localized auxin production in the QC cells. We found that polar auxin transport was affected neither in the *wox5* mutant nor in an ectopic expression of *WOX5* (*35S::WOX5-GR*) (Supplemental Figures 3 and 4). Next, we checked whether WOX5 would contribute to the regulation of local auxin production. Notably, free auxin measurements in *wox5* and *35S::WOX5-GR* plants indicated two antithetic effects on free auxin content of the root. The *wox5* mutant had notably less free IAA in the roots than the control (Figure 4D). Alternatively, *WOX5*-overexpressing plants displayed significantly higher free IAA levels (Figure 4F). This increased free IAA level in *35S::WOX5-GR* was confirmed by higher DR5::GUS signals in roots and young cotyledons (Supplemental Figure 5).

Since WOX5 represents a downstream target for IAA17-repressed auxin responses (Ding and Friml, 2010) (Figure 3), we substantiated our findings by measuring free auxin levels in IAA17 mutants. We found that *35S::VP16-IAA17mImII* plants displayed a decreased free auxin level (Figure 4E), reminiscent of those of *wox5*. In contrast, the *axr3-1* mutant showed a significant increase of free IAA content, similar to that of WOX5-overexpressing plants (Figure 4E).

Taken together, our data suggest that WOX5 modulates either free auxin production or auxin deconjugation and therefore could participate in the maintenance of auxin response maximum in the QC cells. To address this hypothesis, we analyzed the expression level of auxin deconjugation-related genes in the *35S::WOX5-GR* plants. We found that the expression of auxin deconjugation-related genes was not changed after ectopic WOX5 induction (Supplemental Figure 6). Notably, a significant increase of the key auxin biosynthetic gene *YUC1* was observed in WOX5-overexpressing plants (Figure 4G). YUC1 acts downstream of TAA1/WEI8-dependent auxin biosynthesis (Zhao, 2010) and, similarly to *TAA1*, it is preferentially expressed in the QC cells and their proximity (Supplemental Figure 7). Subsequently, we found that the expression of *TAA1* gene was decreased by two-fold in *35S::VP16-IAA17mImII* (Figure 4H) and increased by four-fold in *axr3-1* mutant (Figure 4H). Our results demonstrate that WOX5 is presumably involved in free IAA production by modulating tryptophan-dependent auxin biosynthetic pathway (Zhao, 2010). Taken together, our data reveal the feedback mechanism linking WOX5-mediated auxin production to IAA17-dependent repression of auxin responses in the QC cells.

Simulations of WOX5–IAA17 Feedback Loop Predict Robust Auxin-Maximum Guiding the Patterning of Root Stem Cell Niches

Our experimental data revealed the WOX5–IAA17-dependent feedback mechanism underlying the maintenance of auxin maximal responses in the QC cells that is mediating the patterning of the root DSC niches (Figure 5).

To gain further insights into dynamics of this feedback mechanism, we used a computer modeling approach that integrates the WOX5–IAA17 feedback loop (Figure 5) into our 'flux separation' root model (Figure 1B). To account for the feedback mechanism linking IAA17, WOX5, and auxin production, we made the following experimentally derived assumptions:

(1) WOX5 activity modulates the rate of auxin production in the root (Figure 4I).
(2) IAA17 activity represses cellular auxin response (Figure 2) and thus promotes WOX5 transcription (Figure 4II) (Ding and Friml, 2010).
(3) Auxin promotes proteasome-dependent degradation of IAA17 protein (Chapman and Estelle, 2009) through a canonical TIR1-dependent pathway (Chapman and Estelle, 2009) (Figure 4III).
(4) ARF-mediated cellular auxin responses regulate the *IAA17* transcription (Guilfoyle and Hagen, 2007) (Figure 4VI).

To assure no bias in our model predictions, we assumed that each cell of the root is capable of expressing both IAA17 and

http://doc.rero.ch

http://doc.rero.ch

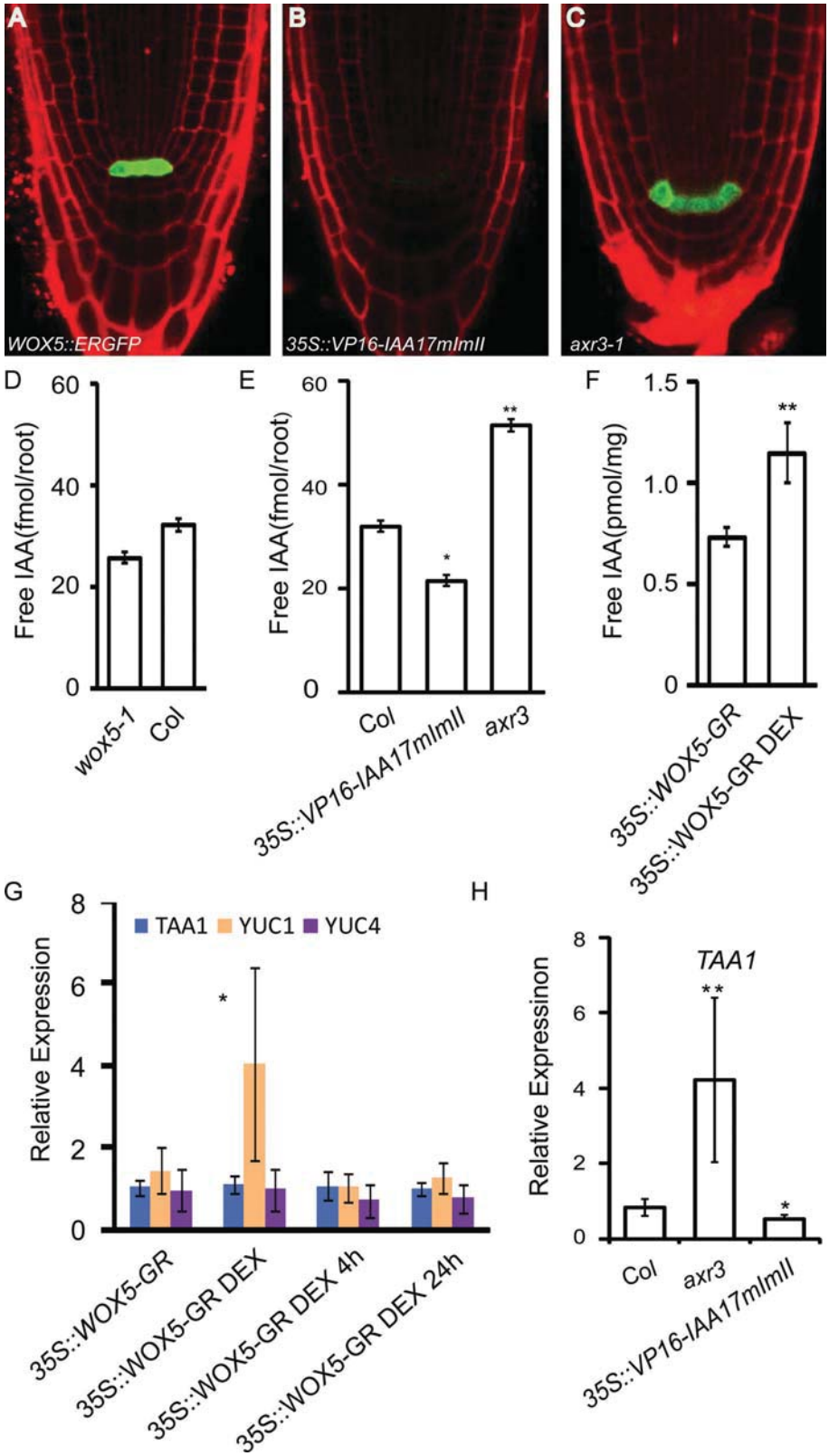

Figure 4. IAA17 Acts Upstream of WOX5-Dependent Modulation of Free Auxin Production.

(A) *WOX5::ERGFP* signal visible solely in the QC cells in the wild-type plants.

(B) Highly repressed *WOX5::ERGFP* signals in the *35S:VP16-IAA17mImII* mutant.

(C) Expanded *WOX5::ERGFP* signals to the endodermis/cortex initials in the *axr3-1* mutant.

WOX5 proteins that are controlled locally by the proposed feedback mechanism. For full mathematical model description, we refer to the Supplemental Methods.

Simulations of our feedback-driven model predicted the highest expression of WOX5 in the QC cells that eventually led to WOX5-mediated auxin production and the maintenance of auxin maximum in these cells (Figure 6A) as observed experimentally (Figure 2A). Moreover, our model predicted the drop of auxin concentrations from the QC cells towards distal columella cells, indicating the formation of steep auxin gradient in the root tip (Figure 6E). Interestingly, the profile of this root tip-associated auxin gradient seems to closely resemble the recent report with a novel auxin biosensor (Brunoud et al., 2012).

We hypothesize that an auxin gradient in the root tip could be instructive for the patterning of root DSC niches. Although an adequate molecular mechanism for the root DSC patterning remains to be investigated, we attempt to epitomize this process by non-linear mapping between auxin concentrations and the level of DSC differentiation (see the Supplemental Methods). With this assumption, our model simulations could reproduce the wild-type-like pattern of root DSC differentiation (Figure 3A). These model predictions were generally robust for fluctuations of parameters such as auxin transport rates (Supplemental Figures 1D–1F), auxin-dependent *IAA17* transcription and IAA17 degradation rates (Supplemental Figure 8), or WOX5-dependent auxin production rates (Supplemental Figure 9).

Next, we performed simulations of *wox5* mutant by setting WOX5 transcription rate to 0 (Figure 6B). Notably, *wox5* simulations predicted all features of the *wox5* mutant (Figures 2 and 3) including the lack of auxin maximum in the QC cells, lower overall auxin levels, and enhanced root DSC differentiation patterns (Figures 2F, 3D, and 6B). A nearly identical phenotype was observed in simulations of *35S::VP16-IAA17mImII* (Figure 6B, 6C, and 6E) that assumed a strong ARF-mediated repression of WOX5 transcription. Interestingly, the opposite phenotype was observed in the simulated IAA17 gain-of-function mutant (*axr3*) that had a lower rate of auxin-mediated degradation of IAA17 protein. The predicted *axr3-1* phenotype displays higher overall auxin levels, clear auxin maximum in the QC cells, broad domain of WOX5 expression, and reduced root DSC differentiation (Figure 6A, 6D, and 6E), therefore reassembling our experimental observations (Figures 2B, 3E, 4C, and 4E).

In conclusion, our model predictions largely agree with *in planta* observations that include predictions of auxin levels, the presumable location of auxin response maximum, WOX5 expression domain, and patterns of root DSC differentiation (Figures 2–4). Therefore, both experimental data and *in silico* computer simulations postulate the feedback mechanism linking WOX5 and IAA17 that controls an auxin gradient-guided patterning of the root tip.

DISCUSSION

Auxin gradients are central to the robust development of the primary root in *Arabidopsis* (Benkova et al., 2003).

Polar auxin transport has been suggested as a minimal mechanism to assure the establishment and maintenance of auxin maximum in the QC of the root (Grieneisen et al., 2007). In addition, localized auxin production and auxin response machinery have been postulated to significantly contribute to this process. Nevertheless, molecular mechanisms underlying localized auxin production and auxin responses during the establishment and maintenance of auxin response maximum in the QC cells are largely uncharacterized.

Here, we addressed these issues by using the combination of experimental and computational modeling approaches. We used the *DR5rev::GFP* reporter for the readout of local auxin gradient across the root tip (Figure 2A). Our experimental observations and model predictions are consistent with other studies using an alternative auxin reporter (DII-Venus) (Band et al., 2012; Brunoud et al., 2012). Our data suggest that QC-localized auxin maximum together with graded auxin concentrations in distal collumella cells behind the QC region (also observed with DII-Venus reporter) (Band et al., 2012; Brunoud et al., 2012) are required to maintain root stem cell identities. We demonstrated that auxin response maximum preferentially localizes to the QC cells and this process requires the IAA17-dependent repression of auxin responses. Consequently, these IAA17-dependent auxin responses restrict the expression domain of WOX5 and therefore maintain the root stem cell identity. Finally, we found that WOX5 modulates free auxin production locally in the QC center, further helping to maintain the high auxin content of QC cells. Our studies highlight WOX5 and IAA17-mediated auxin responses that operate in a feedback-dependent manner to regulate the root DSC differentiation. We found that *axr3-1* displayed enhanced auxin response in QC and reduced auxin response in adjacent columella cells that resulted into the strong inhibition of root DSC differentiation. In contrast,

(D, E) Decreased free IAA levels in the *wox5* mutant (D) and *35S:VP16-IAA17mImII* mutant and significantly increased IAA levels of *axr3-1* mutant (E).
(F) Increase in the free IAA level in *35S::WOX5-GR* seedlings grown on medium with 1 μM DEX inductions.
(G) Long-term induction of WOX5 (seedlings grown on medium with 1 μM DEX) induced YUC1 expression level that was not absent under short-term induction of WOX5 (4-day-old seedlings treated with 10 μM DEX for 4 or 24 h).
(H) Increased expression of TAA1/WEI8 gene in *axr3-1* mutant and slightly decreased expression of TAA1/WEI8 in *35S:VP16-IAA17mImII* mutant compared to the control.
Tubulin is the relative control for Q-PCR analysis. Error bars mark standard errors, from four independent biological repeats (Student's *t*-test, * $P < 0.05$, ** $P < 0.01$).

http://doc.rero.ch

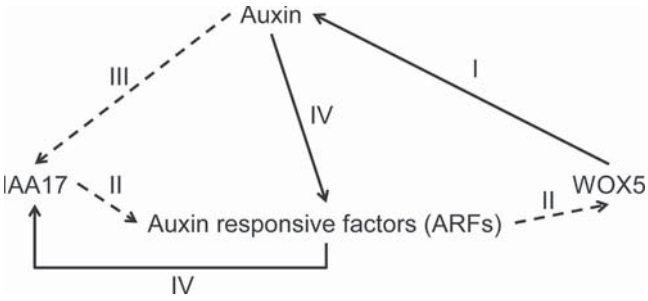

Figure 5. Schematics of WOX5–IAA17 Feedback Mechanism.

Black arrows depict positive regulation and dashed arrows indicate repression mechanism. Greek letters correspond to subsequent computer model assumptions presented in the main text.

activated version of IAA17 in QC cells led to the highly promoted auxin responses in QC and subsequently enhanced differentiation of root stem cells. Additionally, our investigations indicate that a maximum of auxin signaling responses in QC is not sufficient to maintain stem cell identities; it also requires the reduction of auxin responses of adjacent columullar cells. Our data indicate the possibility for auxin response gradient in the root tip that would modulate the patterning of root DSC identity.

Finally, we designed the computer model of this proposed feedback loop that was capable of faithfully reproducing experimental observations, including predictions of auxin levels, auxin distributions, and WOX5 expression and root DSC differentiation patterns. This simplified model that captures the essential features of the feedback regulation between WOX5 and IAA17 was capable of predicting auxin signaling maximum and root DSC differentiation phenotypes which were observed experimentally.

WOX5 has been shown to undergo transcriptional repression by the CLE40/ACR4 signaling cascade derived from the columella cells (De Smet et al., 2008; Stahl and Simon, 2009, 2010). Therefore, it will be interesting to see how this and as-yet unidentified layers of regulation could be further integrated into our model and how this would impact on model predictions and ultimately on our understanding of root patterning processes. Also, future testing of the possibility for the involvement of other AUX/IAA proteins and associated ARF transcription factors in the proposed feedback regulation would substantially extend our understanding of mechanisms underlying root stem cell patterning.

To conclude, our combined experimental and modeling study suggests the unexpected feedback loop that mechanistically link WOX5-dependent auxin production, polar auxin transport, and IAA17-dependent cellular auxin response to facilitate the auxin-maximum guided patterning of root DSC niches. It remains to be tested whether a similar mechanism could be involved in the auxin-dependent patterning of shoots, since WOX5 belongs to the functionally conserved family of major plant stem cell regulators.

METHODS

Plant Materials and Growth Conditions

Published transgenic and mutant lines were: *wox5-1*, *35S::WOX5-GR* (Sarkar et al., 2007), *WOX5::ERGFP* (Xu et al., 2006), *DR5rev::GFP* (Friml et al., 2003), *axr3-1* (mimicking IAA17 repressor) (Sabatini et al., 1999), *35S*::*VP16-IAA17mImII* (representing IAA17 activator) (Li et al., 2009), *PIN3::PIN3::GFP* (Dello Ioio et al., 2008). The *wox5 axr3* double mutant was generated by crossing *wox5-1* with *axr3-1*; *DR5::GUS 35S::WOX5-GR* by crossing *DR5::GUS* with *35S::WOX5-GR*; and *DR5rev::GFP/wox5* and *DR5rev::GFP/35S*:*VP16-IAA17mImII* by crossing *DR5rev::GFP* with *wox5-1* or *35S*::*VP16-IAA17mImII*, respectively. The 2583-bp upstream region from the IAA17 start codon was amplified and linked to the GUS reported in gateway vector PKGWFS7.1 (Karimi et al., 2002) to obtain IAA17Promoter::GUS reporter construct. The *WOX5*::*HA-IAA17mImII* (representing IAA17 repressor) line was generated by replacing the 35S promoter of *35S*::*HA-IAA17mImII* (Li et al., 2009) with the 2583-bp upstream region from the WOX5 start codon. Seeds were surface-sterilized with chlorine gas and incubated for 3 d after being plated onto Murashige and Skoog (MS) medium before transfer to a growth room with a 16-h day/8-h night regime at 19°C for 5 d.

Phenotype Analysis

Starch granules in root tips were stained with Lugol's solution for 1–2 min, mounted onto the slides with chloral hydrate, and checked immediately. Histochemical analysis of β-glucuronidase (GUS) activity was carried out by incubation of seedling roots in GUS staining solution (0.05 M $NaPO_4$ buffer (pH 7.0), 5 mM $K_3Fe(CN)_6$, 5 mM $K_4Fe(CN)_6$, 10 mM X-glucuronide) at 37°C until the blue staining was visible, followed by two washes in distilled water and mounting in 70% (w/v) chloral hydrate and 10% (v/v) glycerol for microscopy. Image acquisition was carried out with an Axiocam HR camera attached to an Olympus microscope. For confocal microscopy images, a Zeiss LSM 510 or Olympus FV10 ASW confocal scanning microscope was used. Cell walls were counterstained by mounting seedling roots in 10 μM propidium iodide.

Immunodetections

The antibodies were diluted as follows: rabbit anti-PIN1 (1:1000), rabbit anti-PIN2 (1:1000; generously provided by C. Luschnig), and Cy3 488-conjugated secondary anti-mouse (1:600; Dianova and Sigma).

Free IAA Measurements

For free IAA contents analysis, approximately 30 roots of respective genotypes were pooled and analyzed in quadruplicates as described earlier (Pencik et al., 2009) or it was quantified as described (Pollmann et al., 2009). For the extraction of plant metabolites, three samples (replicates) of each were incubated at 60°C under constant shaking over 1 h in 1 ml methanol

http://doc.rero.ch

http://doc.rero.ch

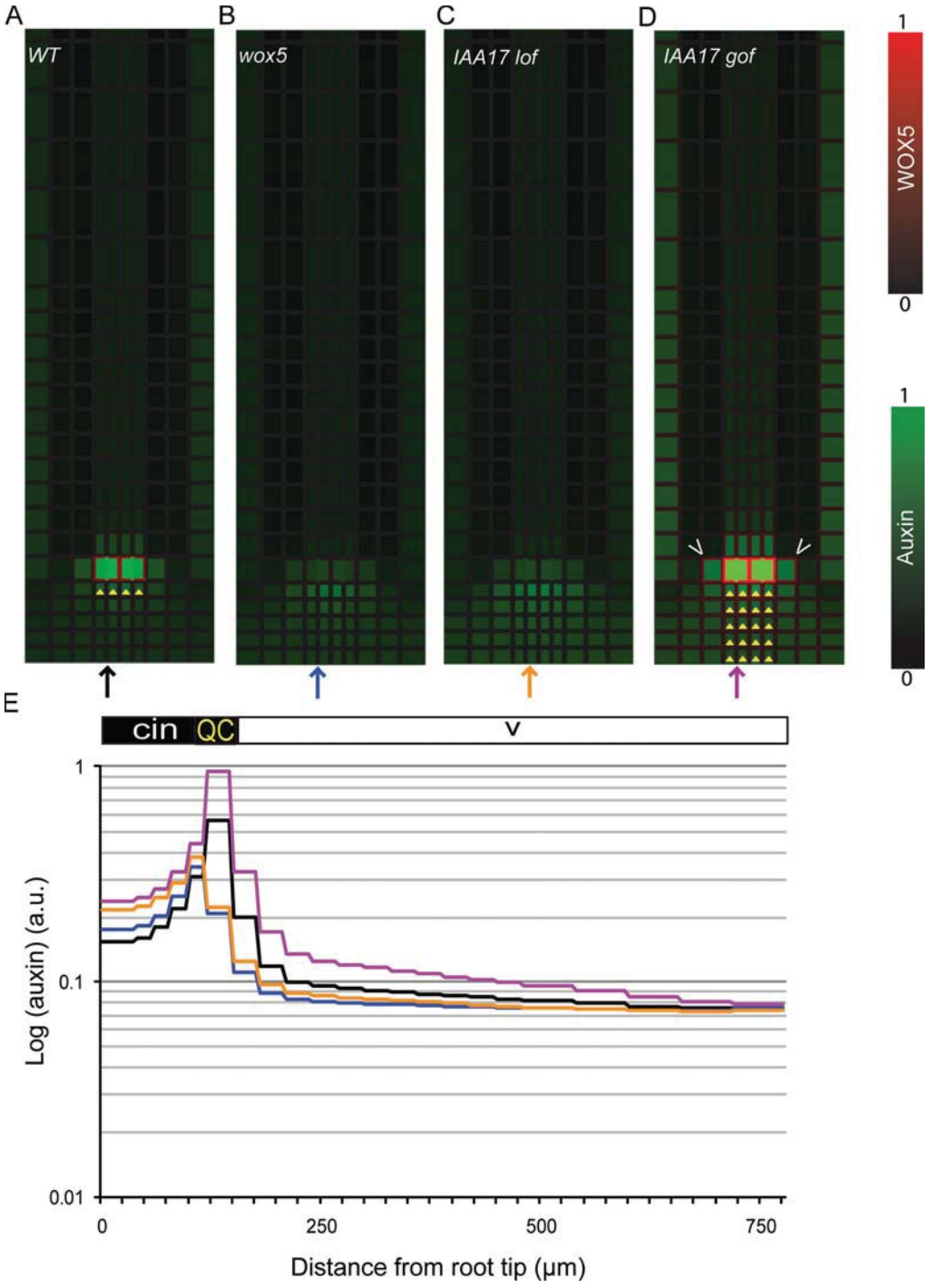

Figure 6. Computer Model Integrates WOX5–IAA17 Feedback Mechanisms to Predict the Patterning of the Root Tip.

(A–D) Compatible *in silico* wild-type simulations of the 'flux separation' model (Figure 1B) that integrates the WOX5–IAA17 feedback loop (A) and the computer simulations of the *in silico wox5* mutant (B), loss of IAA17 function (*35S:VP16-IAA17mImII*) (C), and gain of IAA17 function (*axr3-1*) (D) mutants to experimental observations (Figure 2A–2D). Auxin concentrations are in green and the relative WOX5 expression in red. The predicted WOX5 activities and resulting stem cell layers (depicted by yellow triangles below the QC) correspond to those observed experimentally (Figure 3C–3E).

(E) Steady-state auxin concentration profiles along longitudinal sections through the vascular and columella tissues for wild-type and mutant simulations (distance from root tip in μm). Steep exponential auxin gradients were observed between QC cells and columella initials (cin) in wild-type (black arrowhead) and *axr3-1* (purple green arrow) simulations and were largely absent in the simulations of *wox5* (blue arrow) and *35S:VP16-IAA17mImII* (orange arrow) mutants, similarly to those in experimental measurements (Figure 2). Color coding is for the relative auxin concentrations (green) and relative WOX5 expression (red). Colors of arrows correspond to the auxin gradient profiles.

supplemented with 30 pmol of $[^2H]_2$-IAA (internal standard). Supernatants and residual plant material were separated by centrifugation and the cell-free extracts dried under vacuum. Residues were dissolved in 30 µl methanol to which 200 µl diethyl ether was added. If necessary, dissolving was forced by ultrasonic treatment (Sonorex RK510S, Bandelin, Berlin, Germany). Particle-free samples were loaded onto a custom-made microscale aminopropyl solid-phase extraction cartridge. Columns were washed with 250 µl of $CHCl_3$:2-propanol, 2:1 (v/v), and IAA containing fractions eluted with 400 µl acidified diethyl ether (2% acetic acid (v/v)). Eluates were dried, re-dissolved in 20 µl methanol, and finally derivatized by treatment with 100 µl ethereal diazomethane. Thereafter, samples were transferred into autosampler vials, dried under a gentle stream of nitrogen, and taken up in 15 µl of chloroform. For IAA quantification, 1 µl of the methylated samples was injected into the GC–MS system. The spectra were recorded on a Varian Saturn 2000 ion-trap mass spectrometer coupled with a Varian CP-3800 gas chromatograph (Varian, Walnut Creek, CA, USA). Compounds were separated by chromatography on a ZB-50 fused silica capillary column (Phenomenex, Torrence, CA, USA). The mass spectrometer was used in CI-MRM positive ion detection mode with methanol as the reactant gas. The setting for endogenous IAA was as follows: m/z = 190 $[M+H]^+$ and 0.50 V. In a second channel with the same excitation amplitude, the $[^2H]_2$-IAA standard was analyzed and the setting for the parent ion was: m/z = 192 $[M+H]^+$. The amount of endogenous IAA in the samples was calculated from the signal ratio of the unlabeled over the stable isotope-labeled mass fragment observed in the two analyzed channels.

Quantitative PCR Analysis

RNA was extracted with the RNeasy kit (Qiagen). Poly(dT) cDNA was prepared from total RNA of 5-day-old seedlings. Superscript III reverse transcription (Invitrogen) and quantification were performed on a LightCycler 480 apparatus (Roche Diagnostics) with the SYBR Green I Master kit (Roche Diagnostics) according to the manufacturer's instructions. All individual reactions were performed in triplicate. Data were analyzed with qBase (Hellemans et al., 2007). Expression levels were normalized to those of TUBULIN, which showed no clear systematic changes in Ct value. The primers used to quantify gene expression levels are described in Supplemental Tables 1 and 3.

GUS Staining

Histochemical β-glucuronidase (GUS) staining was performed as described (Friml et al., 2003) overnight at room temperature. Seedlings mounted in chloral hydrate (Fluka) were analyzed with an automatic virtual slide-scanner microscope frame (dotSlide BX51 microscope, Olympus).

Computational Methods

The cellular grid tissue template for the model was created with the version of VV (Vertex-Vertex) programming language (Smith et al., 2006). The simulations were performed by numerical computations of coupled ODE systems, with an adaptive-size, fifth-order Runge-Kutta method. All figures were processed in Adobe Illustrator. Figures 1 and 4 are screenshots from model simulations. Model parameters are described in Supplemental Table 2.

SUPPLEMENTARY DATA

Supplementary Data are available at *Molecular Plant Online.*

FUNDING

This work was supported by funding from: the National Natural Science Foundation of China (No. 31222005 and No. 31270327), the 'Qilu Scholarship' from Shandong University of China and from the Ministry of Education (11200081963024) and '1000-talents Plan' from China for young researchers (11200095551303) to Z.D.; the projects CZ.1.07/2.3.00/20.0043 and CZ.1.05/1.1.00/02.0068 (to CEITEC, Central European Institute of Technology) and the Odysseus program of the Research Foundation-Flanders to J.F.; Youth and Sports of the Czech Republic (MSM6198959216) and the Academy of Sciences of the Czech Republic (KAN200380801) to J.R.; the German Science Foundation (DFG-SFB480/A-10) to S.P.; the Swiss National Science Foundation (Grant No. 31003A-125001), from Research Foundation-Flanders to S.V. (FWO09/PDO/196); and Forschungspool of the University of Fribourg to M.G.

ACKNOWLEDGMENTS

We acknowledge Ben Scheres, Tom J. Guilfoyle, and Thomas Laux sharing published materials and Keke Yi, Jürgen Kleine-Vehn, Seth Davis, and Xu Chen for critical reading of the manuscript. Z.D. and K.W. planned experiments. Z.D., K.W., H.T., T.N., S.P., and J.R. performed experiments. J.F., Z.D., M.G., Z.D., K.W., S.V., W.G., H.L., M.G., and J.F. analyzed the data. Z.D., K.W., and H.T. wrote the paper. No conflict of interest declared.

REFERENCES

Band, L.R., Wells, D.M., Larrieu, A., Sun, J., Middleton, A.M., French, A.P., Brunoud, G., Sato, E.M., Wilson, M.H., Péret, B., et al. (2012). Root gravitropism is regulated by a transient lateral auxin gradient controlled by a tipping-point mechanism. Proc. Natl Acad. Sci. U S A. **109**, 4668–4673.

Benjamins, R., and Scheres, B. (2008). Auxin: the looping star in plant development. Annu. Rev. Plant Biol. **59**, 443–465.

Benkova, E., Michniewicz, M., Sauer, M., Teichmann, T., Seifertova, D., Jurgens, G., and Friml, J. (2003). Local, efflux-dependent auxin gradients as a common module for plant organ formation. Cell. **115**, 591–602.

Bennett, M.J., Marchant, A., Green, H.G., May, S.T., Ward, S.P., Millner, P.A., Walker, A.R., Schulz, B., and Feldmann, K.A.

http://doc.rero.ch

(1996). *Arabidopsis* AUX1 gene: a permease-like regulator of root gravitropism. Science. **273**, 948–950.

Blilou, I., Xu, J., Wildwater, M., Willemsen, V., Paponov, I., Friml, J., Heidstra, R., Aida, M., Palme, K., and Scheres, B. (2005). The PIN auxin efflux facilitator network controls growth and patterning in *Arabidopsis* roots. Nature. **433**, 39–44.

Brunoud, G., Wells, D.M., Oliva, M., Larrieu, A., Mirabet, V., Burrow, A.H., Beeckman, T., Kepinski, S., Traas, J., Bennett, M.J., et al. (2012). A novel sensor to map auxin response and distribution at high spatio-temporal resolution. Nature. **482**, 103–106.

Chapman, E.J., and Estelle, M. (2009). Mechanism of auxin-regulated gene expression in plants. Annu. Rev. Genet. **43**, 265–285.

Cruz-Ramirez, A., Diaz-Trivino, S., Blilou, I., Grieneisen, V.A., Sozzani, R., Zamioudis, C., Miskolczi, P., Nieuwland, J., Benjamins, R., Dhonukshe, P., et al. (2012). A bistable circuit involving SCARECROW-RETINOBLASTOMA integrates cues to inform asymmetric stem cell division. Cell. **150**, 1002–1015.

De Smet, I., Vassileva, V., De Rybel, B., Levesque, M.P., Grunewald, W., Van Damme, D., Van Noorden, G., Naudts, M., Van Isterdael, G., De Clercq, R., et al. (2008). Receptor-like kinase ACR4 restricts formative cell divisions in the *Arabidopsis* root. Science. **322**, 594–597.

Dello Ioio, R., Nakamura, K., Moubayidin, L., Perilli, S., Taniguchi, M., Morita, M.T., Aoyama, T., Costantino, P., and Sabatini, S. (2008). A genetic framework for the control of cell division and differentiation in the root meristem. Science. **322**, 1380–1384.

Ding, Z., and Friml, J. (2010). Auxin regulates distal stem cell differentiation in *Arabidopsis* roots. Proc. Natl Acad. Sci. U S A. **107**, 12046–12051.

Friml, J., Vieten, A., Sauer, M., Weijers, D., Schwarz, H., Hamann, T., Offringa, R., and Jurgens, G. (2003). Efflux-dependent auxin gradients establish the apical–basal axis of *Arabidopsis*. Nature. **426**, 147–153.

Grieneisen, V.A., Xu, J., Maree, A.F., Hogeweg, P., and Scheres, B. (2007). Auxin transport is sufficient to generate a maximum and gradient guiding root growth. Nature. **449**, 1008–1013.

Grunewald, W., and Friml, J. (2010). The march of the PINs: developmental plasticity by dynamic polar targeting in plant cells. EMBO J. **29**, 2700–2714.

Guilfoyle, T.J., and Hagen, G. (2007). Auxin response factors. Curr. Opin. Plant Biol. **10**, 453–460.

Hellemans, J., Mortier, G., De Paepe, A., Speleman, F., and Vandesompele, J. (2007). qBase relative quantification framework and software for management and automated analysis of real-time quantitative PCR data. Genome Biol. **8**, R19.

Ikeda, Y., Men, S., Fischer, U., Stepanova, A.N., Alonso, J.M., Ljung, K., and Grebe, M. (2009). Local auxin biosynthesis modulates gradient-directed planar polarity in *Arabidopsis*. Nat. Cell Biol. **11**, 731–738.

Karimi, M., Inze, D., and Depicker, A. (2002). GATEWAY vectors for Agrobacterium-mediated plant transformation. Trends Plant Sci. **7**, 193–195.

Kepinski, S., and Leyser, O. (2005). The *Arabidopsis* F-box protein TIR1 is an auxin receptor. Nature. **435**, 446–451.

Kleine-Vehn, J., and Friml, J. (2008). Polar targeting and endocytic recycling in auxin-dependent plant development. Annu. Rev. Cell Dev. Biol. **24**, 447–473.

Laskowski, M., Grieneisen, V.A., Hofhuis, H., Hove, C.A., Hogeweg, P., Maree, A.F., and Scheres, B. (2008). Root system architecture from coupling cell shape to auxin transport. PLoS Biol. **6**, e307.

Li, H., Cheng, Y., Murphy, A., Hagen, G., and Guilfoyle, T.J. (2009). Constitutive repression and activation of auxin signaling in *Arabidopsis*. Plant Physiol. **149**, 1277–1288.

Ljung, K., Hull, A.K., Celenza, J., Yamada, M., Estelle, M., Normanly, J., and Sandberg, G. (2005). Sites and regulation of auxin biosynthesis in *Arabidopsis* roots. Plant Cell. **17**, 1090–1104.

Pencik, A., Rolcik, J., Novak, O., Magnus, V., Bartak, P., Buchtik, R., Salopek-Sondi, B., and Strnad, M. (2009). Isolation of novel indole-3-acetic acid conjugates by immunoaffinity extraction. Talanta. **80**, 651–655.

Petersson, S.V., Johansson, A.I., Kowalczyk, M., Makoveychuk, A., Wang, J.Y., Moritz, T., Grebe, M., Benfey, P.N., Sandberg, G., and Ljung, K. (2009). An auxin gradient and maximum in the *Arabidopsis* root apex shown by high-resolution cell-specific analysis of IAA distribution and synthesis. Plant Cell. **21**, 1659–1668.

Pollmann, S., Duchting, P., and Weiler, E.W. (2009). Tryptophan-dependent indole-3-acetic acid biosynthesis by 'IAA-synthase' proceeds via indole-3-acetamide. Phytochemistry. **70**, 523–531.

Sabatini, S., Beis, D., Wolkenfelt, H., Murfett, J., Guilfoyle, T., Malamy, J., Benfey, P., Leyser, O., Bechtold, N., Weisbeek, P., et al. (1999). An auxin-dependent distal organizer of pattern and polarity in the *Arabidopsis* root. Cell. **99**, 463–472.

Sarkar, A.K., Luijten, M., Miyashima, S., Lenhard, M., Hashimoto, T., Nakajima, K., Scheres, B., Heidstra, R., and Laux, T. (2007). Conserved factors regulate signalling in *Arabidopsis thaliana* shoot and root stem cell organizers. Nature. **446**, 811–814.

Smith, K.J., Barnato, A.E., and Roberts, M.S. (2006). Teaching medical decision modeling: a qualitative description of student errors and curriculum responses. Med. Decis. Making. **26**, 583–588.

Stahl, Y., and Simon, R. (2009). Is the *Arabidopsis* root niche protected by sequestration of the CLE40 signal by its putative receptor ACR4? Plant Signal Behav. **4**, 634–635.

Stahl, Y., and Simon, R. (2010). Plant primary meristems: shared functions and regulatory mechanisms. Curr. Opin. Plant Biol. **13**, 53–58.

Stepanova, A.N., Robertson-Hoyt, J., Yun, J., Benavente, L.M., Xie, D.Y., Dolezal, K., Schlereth, A., Jurgens, G., and Alonso, J.M. (2008). TAA1-mediated auxin biosynthesis is essential for hormone crosstalk and plant development. Cell. **133**, 177–191.

Swarup, R., Kramer, E.M., Perry, P., Knox, K., Leyser, H.M., Haseloff, J., Beemster, G.T., Bhalerao, R., and Bennett, M.J. (2005). Root gravitropism requires lateral root cap and epidermal cells for transport and response to a mobile auxin signal. Nat. Cell Biol. **7**, 1057–1065.

Tao, Y., Ferrer, J.L., Ljung, K., Pojer, F., Hong, F., Long, J.A., Li, L., Moreno, J.E., Bowman, M.E., Ivans, L.J., et al. (2008). Rapid synthesis of auxin via a new tryptophan-dependent pathway is required for shade avoidance in plants. Cell. **133**, 164–176.

Vanneste, S., and Friml, J. (2009). Auxin: a trigger for change in plant development. Cell. **136**, 1005–1016.

http://doc.rero.ch

Vernoux, T., Brunoud, G., Farcot, E., Morin, V., Van den Daele, H., Legrand, J., Oliva, M., Das, P., Larrieu, A., Wells, D., et al. (2011). The auxin signalling network translates dynamic input into robust patterning at the shoot apex. Mol. Syst. Biol. **7**, 508.

Wabnik, K., Govaerts, W., Friml, J., and Kleine-Vehn, J. (2011). Feedback models for polarized auxin transport: an emerging trend. Mol. Biosyst. **7**, 2352–2359.

Woodward, A.W., and Bartel, B. (2005). Auxin: regulation, action, and interaction. Ann. Bot. **95**, 707–735.

Xu, J., Hofhuis, H., Heidstra, R., Sauer, M., Friml, J., and Scheres, B. (2006). A molecular framework for plant regeneration. Science. **311**, 385–388.

Zhao, Y. (2010). Auxin biosynthesis and its role in plant development. Annu. Rev. Plant Biol. **61**, 49–64.

http://doc.rero.ch